# Rigorous Modeling of Fixed-Bed Reactors Containing Finite Hollow Cylindrical Catalyst with Michaelis-Menten Type of Kinetics

Mohammad Asif

*Abstract*—A large number of chemical, bio-chemical and pollution-control processes use heterogeneous fixed-bed reactors. The use of finite hollow cylindrical catalyst pellets can enhance conversion levels in such reactors. The absence of the pellet core can significantly lower the diffusional resistance associated with the solid phase. This leads to a better utilization of the catalytic material, which is reflected in the higher values for the effectiveness factor, leading ultimately to an enhanced conversion level in the reactor. It is however important to develop a rigorous heterogeneous model for the reactor incorporating the two-dimensional feature of the solid phase owing to the presence of the finite hollow cylindrical catalyst pellet. Presently, heterogeneous models reported in the literature invariably employ one-dimension solid phase models meant for spherical catalyst pellets. The objective of the paper is to present a rigorous model of the fixed-bed reactors containing finite hollow cylindrical catalyst pellets. The reaction kinetics considered here is the widely used Michaelis–Menten kinetics for the liquid-phase bio-chemical reactions. The reaction parameters used here are for the enzymatic degradation of urea. Results indicate that increasing the height to diameter ratio helps to improve the conversion level. On the other hand, decreasing the thickness is apparently not as effective. This could however be explained in terms of the higher void fraction of the bed that causes a smaller amount of the solid phase to be packed in the fixed-bed bio-chemical reactor.

*Keywords*—Fixed-bed reactor, Finite hollow cylinder, Catalyst pellet, Conversion, Michaelis-Menten kinetics.

## I. INTRODUCTION

HETEROGENEOUS fixed-bed reactors often constitute the core of chemical, biochemical, food, refinery and pollution control processes. Its performance is therefore crucial for the overall economics of the process. Any attempt towards the optimal design of the any catalytic reactor begins with a rigorous model of the heterogeneous reactor. Of particular importance in this connection is the optimal design of the catalyst itself by considering the size of the catalyst, its shape and the distribution of the active material inside the permeable porous solid support. The transport of the reactant inside the porous network of the catalyst pellet occurs by the diffusion phenomenon. Due to the mass transport resistance however, the concentration of the reactant gradually decreases towards the interior of the catalyst pellet. The regions deep inside the catalyst are thus exposed to a much lower concentration of the reactant. Due to the occurrence of the concentration gradients inside the catalyst pellet, the rate of

M. Asif is with King Saud University, Riyadh 11421, Saudi Arabia. (phone: 966-1-467-6849; fax: 966-1-467-8770; e-mail: masif@ksu.edu.sa).

the reaction is also similarly affected. Regions with lower concentration of the reactant possess lower reaction rates while it is only the surface of the catalyst pellet that possesses the highest rate of reaction. The net result of this phenomenon is an inefficient utilization of the catalytic material. It is therefore important towards the optimization of the catalyst to design the shape of the pellet itself in such a way that the regions with low concentration of the reactant can be eliminated. The most suitable geometry towards this end is the hollow cylindrical; where of the core of the cylinder is removed thereby minimizing the effect of the internal mass transport resistance. This will enhance the overall effectiveness of the catalyst pellet, and will lead to an improved efficiency of the heterogeneous reactor configurations. The distribution of the active catalytic component is assumed to be uniform throughout the porous structure. The objective of the present study is to develop a detailed rigorous model for a heterogeneous fixed bed reactor that contains the solid catalyst pellet of hollow cylindrical shape instead of the commonly used spherical shape. The kinetics considered here is an important biochemical Michaelis-Menten type of reaction kinetics.

## II. LITERATURE REVIEW

There are several issues that need to be considered towards the optimal design of the catalyst pellet. This includes the size of the pellet itself. A pellet of small size, for example, can always help to lower the effect of the internal mass transport resistance. Another important aspect is the shape of the catalyst pellet. Most non-spherical shapes tend to possess higher effectiveness factor as compared to spherical pellets of the same volume owing to greater surface areas possessed by particles of non-spherical shape[1–2]. Another aspect that has attracted a lot of attention is the deliberate non uniform distribution of the catalytic material within the support. This aspect has been an active research since early sixties [3–6]. For example, it was shown by Mars and Gorgels [3] that catalyst pellets that possess an inert core show better selectivity during selective hydrogenation of acetylene. On the other hand, it was shown by Kosaoka and Sakata [6] that higher effectiveness factors are obtained for slabs with a declining catalytic activity distribution towards the interior of the catalyst. It is interesting to note the effect of the order of the reaction on the effectiveness factor in the case of the non-uniform distribution of the catalytic activity. It was reported that non-uniform distribution can help to improve the

effectiveness factor for different types of reaction kinetics [7–11]. An important contribution in this area was made by Morbidelli et al. [12]. They showed that the optimal catalyst distribution is an appropriately chosen Dirac-delta function for a fixed amount of the catalytic material. This means that the active catalyst should be located at a specific position within pellet. Their findings were supported by numerous other researchers for various types of reaction kinetics [13-16]. In this context, it is important to note the limitations pointed out by Armor as far as the actual commercial implementation of the Dirac-delta type catalytic activity distribution is concerned [17-18].

Another approach recently suggested in the literature is to design the catalyst matrix by mixing materials of two different diffusivities. The idea is to improve the diffusivity of the catalytic material by adding material of high diffusivity such that the resultant diffusivity of the product is much higher than the actual catalytic material [19-22].

It has been recently pointed out by Asif [23] that a non-spherical catalytic support is preferable over a spherical one since the former provides a greater surface area than the latter for any given volume. The author was clearly able to show that a substantial improvement in the effectiveness factor is obtained using hollow cylindrical catalyst pellets. It is therefore important to present a rigorous heterogeneous reactor model that can be used to optimize the conversion level in a fixed bed reactor.

### III. MATHEMATICAL MODEL

The main features of the model presented in the following are similar to those recently discussed by Asif [23]. The difference lies in the reaction kinetics. The present model is based on the Michaelis-Menten type of reaction kinetics, which is commonly encountered in liquid-phase biochemical reactions. The particular reaction considered here is the decomposition of the urea. The proposed model accounts for the presence of both the mass transport mechanisms of the dispersion as well as the convection in the fluid phase. The reactant concentration gradients in the fluid phase exist only in the axial direction. On the other hand, the solid phase in the present model comprises of finite hollow cylindrical catalyst pellets, where concentration gradients exist both in the axial as well as the radial directions due to the presence of internal mass transport (diffusional) resistances. The presence of the film or the external mass transport resistance at the interface of the solid and liquid phase is also accounted in the problem formulation.

#### A. Model for Solid Phase with Michaelis-Menten Type of Reaction Kinetics

The two-dimensional partial differential equation governing the reactant concentration distribution inside the solid catalyst pellet is given by

$$D_r \frac{1}{r}\frac{\partial}{\partial r}\left(r\frac{\partial C_{As}}{\partial r}\right) \;+\; D_z \frac{\partial^2 C_{As}}{\partial z^2} \;-\; R_x(C_{As}) \;=\; 0 \qquad (1)$$

At the solid-fluid interface, the film mass transport resistances are accounted using the following boundary conditions are,

$$At\ r = R_i, \quad D_r\left(\frac{\partial C_{As}}{\partial r}\right) = k_m\left(C_{As} - C_{Af}\right) \qquad (2a)$$

$$At\ r = R_o, \quad -D_r\left(\frac{\partial C_{As}}{\partial r}\right) = k_m\left(C_{As} - C_{Af}\right) \qquad (2b)$$

$$At\ z = 0, \quad \left(\frac{\partial C_{As}}{\partial z}\right) = 0 \qquad (2c)$$

$$At\ z = (H/2), \quad -D_z\left(\frac{\partial C_{As}}{\partial z}\right) = k_m\left(C_{As} - C_{Af}\right) \qquad (2d)$$

where, $C_{As}$ and $C_{Af}$ are the reactant concentration in the solid phase and fluid phase, respectively. $D_r$ and $D_z$, are effective diffusivities in $r$ and $z$ directions, respectively. $R_x(C_{As})$ is the generalized rate of the reaction For the hollow cylindrical catalyst pellet, $H$ is the height, $R_i$ and $R_o$ are inner and outer radii, respectively. $k_m$ is the mass transfer coefficient. Note that the boundary conditions imposed account for the film mass transfer resistance.

Introducing the following dimensionless variables,

$$u = \frac{C_{As}}{C_{Afo}}; \quad \rho = \frac{r}{R_o}; \quad \xi = \frac{z}{(H/2)}; \quad \gamma_o = \frac{(H/2)}{R_o};$$

$$\kappa = \frac{R_i}{R_o}; \quad \gamma^2 = \frac{D_r}{D_z}\gamma_0^2; \quad Sh = \frac{k_m R_o}{D_e} \qquad (3)$$

Note that the height to diameter ratio ($\gamma_o$) and thickness ($\kappa$) are two important shape factors that determine the shape of a hollow cylindrical catalyst pellet. A high value of $\gamma_o$ means a long catalyst while $\kappa = 0$ is a solid cylinder, and $\kappa \to 1$ indicates a very thin hollow cylinder. Rewriting the differential equation and associated boundary conditions in the dimensionless form:

$$\frac{1}{\rho}\frac{\partial}{\partial \rho}\left(\rho\frac{\partial u}{\partial \rho}\right) \;+\; \frac{1}{\gamma^2}\left(\frac{\partial^2 u}{\partial \xi^2}\right) \;-\; \phi_x^2 f_x(u) \;=\; 0 \qquad (4)$$

$$At \quad \rho = \kappa; \quad -\frac{1}{Sh}\left(\frac{\partial u}{\partial \rho}\right) + u = v \ \text{for all}\ \xi \qquad (5a)$$

$$At \quad \rho = 1; \quad \frac{1}{Sh}\left(\frac{\partial u}{\partial \rho}\right) + u = v \ \text{for all}\ \xi \qquad (5b)$$

$$At \quad \xi = 0; \quad \frac{\partial u}{\partial \xi} = 0 \ \text{for all}\ \rho \qquad (5c)$$

$$At \quad \xi = 1; \quad \frac{\gamma_0}{\gamma^2 Sh}\left(\frac{\partial u}{\partial \xi}\right) + u = v \ \text{for all}\ \rho \qquad (5d)$$

where,

$$R_x(w) = \frac{V_{max} w}{(K_m + w)}; \quad \phi_x^2 = \left( \frac{R_x(C_{Afo})R_o^2}{C_{Afo}D_r} \right)$$

$$f_x(u) = \frac{R_x(u C_{Afo})}{R_{xo}(C_{Afo})} = \frac{(K_m + C_{Afo})u}{(K_m + u C_{Afo})}$$
(6)

where $C_{Af0}$ is the inlet feed concentration while $V_{max}$ and $K_m$ are reaction rate parameters.

The corresponding problem for the spherical geometry can be written as:

$$\frac{1}{\rho^2}\frac{\partial}{\partial \rho}\left( \rho^2 \frac{\partial u}{\partial \rho} \right) - \phi_x^2 f_x(u) = 0$$
(7)

$$At\ \rho = 0; \quad \left( \frac{\partial u}{\partial \rho} \right) = 0$$
(8a)

$$At\ \rho = 1; \quad \frac{1}{Sh}\left( \frac{\partial u}{\partial \rho} \right) + u = v$$
(8b)

### B. Model for the Fluid Phase [23]

The fluid phase modeling equations are essentially same as presented before [23]. Yet the detailed derivation is once again presented here in order to make the present paper self-contained.

The differential equation governing the axial distribution of the concentration of the reactant A in the fluid phase ($C_{Af}$) is given by,

$$\varepsilon\left[ \frac{\partial C_{Af}}{\partial t} \right] = -\left[ \frac{\partial}{\partial z}\left( -D_{Az}\frac{\partial C_{Af}}{\partial z} + U C_{Af} \right) \right] + \frac{(1-\varepsilon)}{V_P}W_A$$
(9a)

where, $\varepsilon$ is the fraction of solid phase per unit bed volume, $V_p$ is the volume of the catalyst pellet, $U$ is the local fluid superficial velocity, $D_{Az}$ is the fluid phase dispersion coefficient. Here, the molar flow ($W_A$) of the reactant to the solid catalyst pellet, in terms of the rate of the reaction ($R_x$), is given by,

$$W_A = \iiint R_x(C_{As})dV = \int_0^{2\pi}\int_{-H/2}^{H/2}\int_{R_i}^{R_o} R_x(C_{As})r\,dr\,dz\,d\theta$$
(9b)

where, $C_{As}$ is the concentration distribution of the reactant A in the solid phase comprising of the hollow cylindrical catalyst pellet of height $H$, and $R_i$ and $R_o$ being the internal and outer radii, respectively.

Introducing the dimensionless variables in (9a),

$$\tau = \frac{U_o t}{\varepsilon L}; \quad Pe = \frac{U_o L}{D_{Az}}; \quad v = \frac{C_{Af}}{C_{Afo}}; \quad x = \frac{z}{L};$$
(9c)

and rearrangement leads to,

$$\frac{\partial v}{\partial \tau} = \frac{1}{Pe}\frac{\partial^2 v}{\partial x^2} - \frac{\partial v}{\partial x} + (1-\varepsilon)\frac{L}{U_o}\left( \frac{W_A}{C_{Afo}V_p} \right)$$
(10a)

where, the Peclet number ($Pe$) is a measure of the degree of the back-mixing prevailing in the reactor. For long reactors, $Pe$ is large and the effect of the fluid back-mixing is negligible. Recalling that the molar flow to the catalyst pellet depends upon the average rate of the reaction inside the catalyst pellet, the fluid-solid interaction term in (10a) can be written as,

$$\left( \frac{W_A}{V_p} \right) = \frac{2}{1-\kappa^2}\int_0^1\int_\kappa^1 R_x(C_{As})\rho\,d\rho\,d\xi$$
(10b)

The steady-state counterpart of (10a) can now be rewritten as,

$$\frac{1}{Pe}\left[ \frac{d^2 v}{dx^2} \right] - \frac{dv}{dx} + (1-\varepsilon)\frac{L}{U_o}\frac{R_{x0}}{C_{Afo}}\frac{2}{1-\kappa^2}\int_0^1\int_\kappa^1 f_x \rho\,d\rho\,d\xi = 0$$
(11a)

where,

$$R_{x0} = R_x(C_{Afo})$$
(11b)

is the rate of reaction evaluated at the feed conditions. Defining the effectiveness factor ($\eta$) and the Damkohler number ($Da$) as follows:

$$Da = \left( \frac{L R_{xo}}{U_o C_{Afo}} \right) = \left( \frac{L}{U_o}\frac{V_{max}}{K_m + C_{Afo}} \right)$$
(12)

$$\eta = \frac{2}{1-\kappa^2}\int_0^1\int_\kappa^1 f_x \rho\,d\rho\,d\xi$$

Therefore, (11a) can be written as,

$$\frac{1}{Pe}\left[ \frac{d^2 v}{dx^2} \right] - \frac{dv}{dx} + (1-\varepsilon)Da\,\eta = 0$$
(13)

The widely used boundary condition can be rewritten as,

$$At\ x = 0; \quad -\frac{1}{Pe}\left( \frac{dv}{dx} \right) + v = 1$$
(14a)

$$At\ x = 1; \quad \frac{dv}{dx} = 0$$
(14b)

### IV. RESULTS AND DISCUSSION

The example used here is the enzymatic conversion of urea using the urease enzyme, which catalyzes the degradation of urea to ammonia and carbamine acid. The acid decomposes to

produce another molecule of ammonia and carbon dioxide. As shown in Fig. 1a, the reaction scheme for the formation of ammonia and carbamine acid is given as:
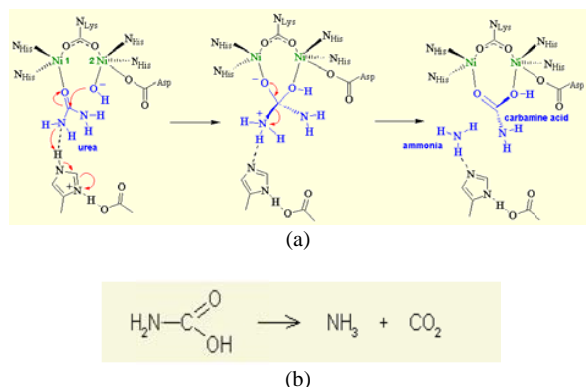


(a)



(b)

Fig. 1 (a) Reaction scheme for the formation of ammonia and carbamine acid (b) Reaction scheme for the formation of ammonia and carbon dioxide

On the other hand, the carbamine acid decomposes spontaneously to form ammonia and carbon dioxide as shown in Fig. 1b.

The reaction kinetics for the above reaction scheme can be represented by the Michaelis-Menten type kinetics as follows:

$$R_{urea} = -\frac{V_{max}C_{urea}}{\left(K_m + C_{urea}\right)} \quad (15)$$

where, units of the rate of reaction is (kmol/m$^3$.s) and those of $C_{urea}$ are (kmol/m$^3$). The reaction parameters are $V_{max}$= 0.067 (kmol/m$^3$.s), $K_m$= 0.0266 (kmol/m$^3$) while the initial urea concentration is taken $C_{Af0}$ = 0.20 (kmol/m$^3$).

In the present, the validity of the numerical code is first tested by using the analytical solution for the linear kinetics. This was achieved by modifying the kinetic parameters by assigning $V_{max}$ = 1.33 and $K_m$ = 2.66. This led to $\phi_V$ being 6.85. For this value of the Thiele modulus, the effective factor for the corresponding spherical and hollow cylindrical catalyst pellet was 0.35 and 0.61, respectively. The conversion profiles are presented in Fig. 2 using 41 grid points. The run with 21 grid points showed convergence problem. Runs were made using 31, 41 and 81 grid points both in the axial as well as radial directions. The required CPU times were 7.931069 s, 10.319631 s and 23.284904 s, respectively on a laptop with Intel Core i7-2640M, 2.80 GHz processor. As far as solution accuracy was concerned, there was hardly any difference in the result. All the subsequent runs were therefore made using 41 grids.
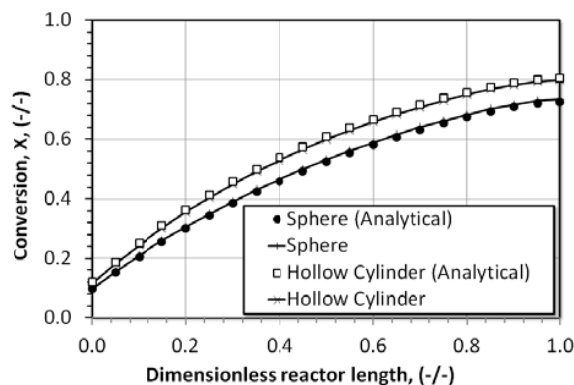


Fig. 2 Comparison of numerical and analytical solutions for the Michaelis-Menten type urea decomposition kinetics using 41 grids in the axial and radial directions of the hollow cylindrical catalyst pellet

TABLE I
REACTION KINETICS AND REACTOR CONDITIONS OF THE UREA DECOMPOSITION

| | |
|---|---|
| Catalyst diameter ($D_V$) | 6.35 mm |
| Shape parameter for hollow spherical catalyst pellets | $\kappa = 0.5, \gamma_o = 1$ |
| Equivalent specific surface radius, $R_{sv}$ | 1.83e-003 |
| Outside radius, $R_o$ | 3.05e-003 |
| Bed void fraction, $\varepsilon$ | 0.45 |
| Bed porosity, $\varepsilon_{HC}$ | 0.59 |
| Effective diffusivity, $D_e$ | 1.0e-07(m$^2$.s$^{-1}$) |
| Fluid velocity, $U_o$ | 0.025 (m/s) |
| Thiele modulus, $\phi_V = \left(\dfrac{R_x(C_{Afo})R_V^2}{C_{Afo}D_e}\right)^{0.5}$ | 5.44 |
| Effectiveness factor, $\eta_{HC}$ | 0.86 |
| Damkohler number, $Da$ | 1.9 |
| Sherwood number, $Sh$ | 100 |
| Peclet number, $Pe$ | 12 |

Using the parameter values reported in the Table I, the governing differential equations were solved, and the predictions are shown in Fig. 3. It is clear that the hollow cylindrical pellets show improved conversion. The conversion is about 8.5% higher for the hollow cylinder as compared to spherical ones. Another feature of the plot seen here is a finite amount of conversion at the reactor inlet. This is due to the incorporation of the dispersion effects in the reactor. This is worthwhile to point out that the dispersion can often be ignored for high fluid velocity and long reactors. The influence of the liquid back-mixing or the dispersion in the present liquid–phase reactor cannot be ignored in view of the fact that the reactor lengths are often short. Note that the boundary at the reactor inlet conforms to the well-known Dancwert's boundary conditions.
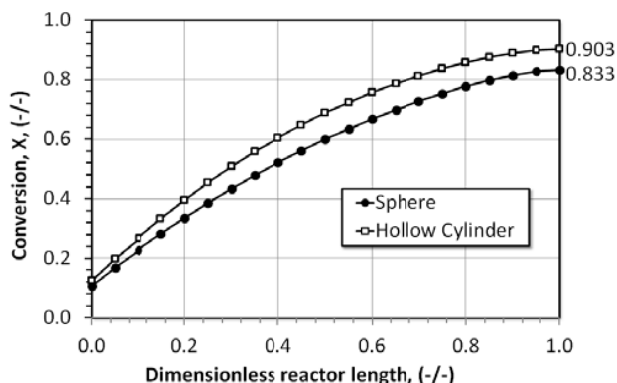
Fig. 3 Conversion profile for the conversion for heterogeneous model using hollow cylindrical catalyst pellet and spherical pellet for ($\gamma_o$) = 1 for κ = 0.5

Two more simulation runs were further carried out by varying the height-to-diameter ratio. For $\gamma_o$ = 0.10, the results are presented in Fig. 4. The conversion is better than the previous case of $\gamma_o$ = 1. The improvement is now 11% as compared to a solid sphere. On the other hand, the conversion reaches as high as 0.976 using $\gamma_o$ = 10, which is a significant enhancement in the conversion level. The reactor profiles for the spherical as well as the hollow cylindrical pellets are shown in Fig. 5. The improvement is now 17%. Note that 83% conversion in this case is reached with half the reactor length. It is clear that higher conversions are obtained using long hollow cylinders as compared to short ones.
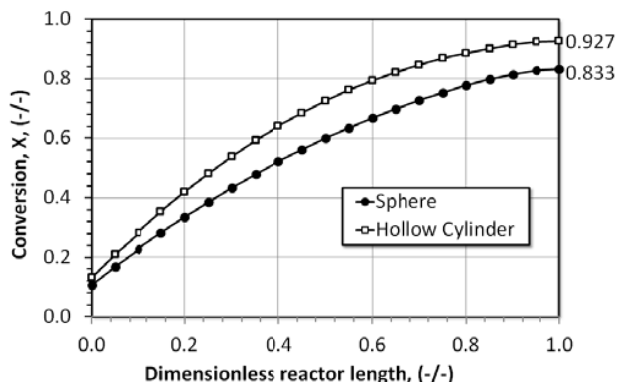


Fig. 4 Conversion profile for the conversion for heterogeneous model using hollow cylindrical catalyst pellet and spherical pellet for ($\gamma_o$) = 0.1 for κ = 0.5
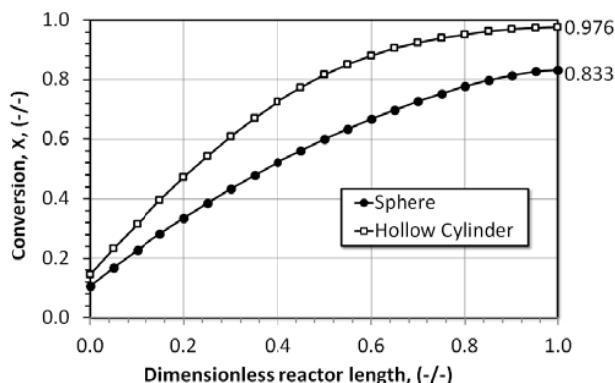
Fig. 5 Conversion profile for the conversion for heterogeneous model using hollow cylindrical catalyst pellet and spherical pellet for ($\gamma_o$) = 10 for κ = 0.5

The effect of both the shape parameters, i.e. $\gamma_o$ as well as κ, are shown in Fig. 6. The effect of the height to diameter ratio was already clear from the foregoing discussion. On the other hand, the effect of the thickness appears a little less critical. The conversion level for κ = 0.3 and κ = 0.5 are almost same whilst the one with κ = 0.7 appear to yield a lower conversion level. In this connection, it however important to note that bed void fractions in these cases are quite different due to the difference in the catalyst thickness. For κ = 0.0, 0.30, 0.50 and 0.70, the bed void fractions are 0.45, 0.50, 0.59, 0.72, and the effectiveness factors are 0.65, 0.78, 0.88, 0.95, respectively. It is therefore clear that increasing the κ from 0.3 to 0.5 helps increasing the effectiveness factor by almost 13% while increasing the κ from 0.5 to 0.7 yields a relatively smaller enhancement of 8% in the effectiveness factor. Moreover, any further increase in κ will not be useful as the effectiveness factor is already close to unity. There is nevertheless another important issue that need to be carefully examined. This relates to the bed void fraction. The percent increase in the voidage is 18% for the change in κ from 0.3 to 0.5 while the change in κ from 0.5 to 0.7 yields a 22% increase in the bed void fraction. A greater bed void means a less volume of the solid catalytic material. The lowering of the bed conversion level in Fig. 6 is therefore due to the lesser quantity of the catalytic material present in the bed.
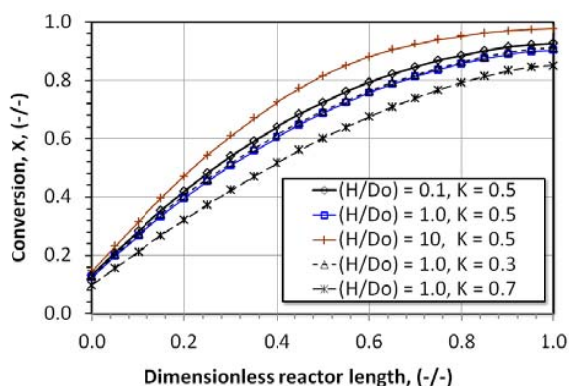


Fig. 6 Effect of shape parameters on the level of conversion

## V. Conclusion

A rigorous model is presented here for the fixed-bed bioreactor containing finite hollow cylindrical catalyst pellets. The model is capable of describing the convection as well as the dispersion in the liquid phase. Both the internal as well as the external mass transport resistances are accounted in the modeling of the solid phase which comprises of finite hollow cylindrical catalyst pellets. Several runs were made to examine the improvement in the conversion level in the fixed bed reactor using the finite hollow cylindrical pellets as compared to the spherical pellets. In all cases, a significant improvement was observed. A greater conversion level is obtained using long pellets as compared to short ones. On the other hand, the effect of the thickness of the hollow cylindrical catalyst pellet was not so substantial. This is attributed to a significant rise in the bed void fraction than a corresponding increase in the effectiveness factor.

## Acknowledgment

## References

[1] Bird, R.B., Stewart, W.E., and Lightfoot, E.N. Transport Phenomena, 2nd Ed. John Wiley & Sons, Inc. 2002.
[2] Aris, R., The optimal design of chemical reactors: a study in dynamic programming. Academic Press, 1961
[3] Mars, P. and Gorgels, M. J., 1964, Hydrogenation of acetylene -a theory of selectivity. In Chemical Reaction Engineering: Proceedings of the Third European Symposium, Supplement to Chem. Eng. Sci., pp. 55-65. Oxford: Pergamon Press.
[4] Michalko, E., 1966a, Method for oxidizing gaseous combustible waste products, U.S. Patent 3,259,454.
[5] Michalko, E.,1966b, Preparation of catalyst for the treatment of combustible waste products, U.S. Patent 3,259,589.
[6] Kasaoka, S. and Sakata, Y., 1968, Effectiveness factors for non-uniform catalyst pellets, J. Chem. Eng. Japan 1: 138-142.
[7] Villadsen, J. and Michelsen, M.J., 1978, Solution of Differential Equations Models by Polynomial Approximation, Prentice-Hall, New Jersey
[8] Becker, E. R. and Wei, J., 1977, Non-uniform distribution of catalysts on supports. Bimolecular Langmuir reactions, J. Catal. 46: 365-371.
[9] Juang, H.-D. and Weng, H.-S., 1983. Performance of catalysts with non-uniform activity profiles 2. Theoretical analysis for non-isothermal reactions. Ind. Eng. Chem. Fundam. 22: 224-230.
[10] Johnson, D. L., and Verykios, X. E., 1983, Selectivity enhancement in ethylene oxidation employing partially impregnated catalysts, J. Catal. 79: 156-163.
[11] Johnson, D. L., and Verykios, X. E., 1984, Effects of radially non-uniform distributions of catalytic activity on performance of spherical catalyst pellets, AI.ChEJ. 30: 44-50.
[12] Morbidelli, M., Servida, A. and Varma, A., 1982, Optimal catalyst activity profiles in pellets 1. The case of negligible external mass transfer resistance, Ind. Eng. Chem. Fundam. 21: 278-284.
[13] Morbidelli, M., Gavriilidis, A. and Varma, A., 2001, Catalyst design, Optimal distribution of catalyst in pellets, reactors and membranes, Cambridge University Press, Cambridge, UK.
[14] Wu, H., Brunovska, A., Morbidelli, M. and Varma, A., 1990, Optimal catalyst activity profiles in pellets VIII. General nonisothermal reacting systems with arbitrary kinetics, Chem. Eng. Sci. 45: 1855-1862; 46: 3328-3329.
[15] Baratti, R., Gavriilidis, A., Morbidelli, M., and Varma, A., 1994, Optimization of a non-isothermal non-adiabatic fixed-bed reactor using Dirac-type silver catalysts for ethylene epoxidation, Chem. Eng. Sci. 49: 1925-1936
[16] Hwang, S., Linke, P. and Smith, R., 2004, Heterogeneous catalytic reactor design with optimum temperature profile II: application o non-uniform catalyst, Chem. Eng. Sci. 59: 4245-4260.
[17] Armor, J.N., 2005, Do you really have a better catalyst? Appl. Catal. A: General 282: 1-4.
[18] Khanaev, V.M., Borisova, E.S. and Noskov, A.S., 2004, Optimization of the active component through the catalyst bed, Chem. Eng. Sci. 59: 1213-1220.
[19] Wei, J. 2011, Catalyst designs to enhance diffusivity and performance-I: Concepts and analysis, Chem. Eng. Sci. 66: 4382-4388.
[20] Wang, G., Coppens, M.-O., 2010. Rational design of hierarchically structured porous catalysts for autothermal reforming of methane. Chem. Eng. Sci. 65:2344.
[21] Wang, G., Johannessen, E., Kleijn, C.R., deLeeuw, S.W., Coppens, M.-O., 2007, Optimizing transport in nano structured catalysts: a computational study, Chem. Eng. Sci. 62: 5110-5118.
[22] Ying, J., Garcia Martinez, J., 2009, Mesostructured zeolitic materials, and methods of making and using them.US Patent US7,589,041 B2, issued September 15, 2009.
[23] Asif, M., 2012, Conversion in Chemical Reactors using Hollow Cylindrical Catalyst Pellet, International Journal of Chemical and Environmental Engineering 6: 178-183.